

1

2 PROFESSOR TIANZHEN ZHANG (Orcid ID : 0000-0001-7873-4547)

3 DR YAN HU (Orcid ID : 0000-0003-1680-8269)

4

5

6 Article type : Original Article

7

8

9 **Identification and characteristics of a novel gland-forming gene in the**  
10 **cotton**

11

12 Yihao Zang<sup>1\*</sup>, Chenyu Xu<sup>1\*</sup>, Lisha Xuan<sup>1</sup>, Lingyun Ding<sup>2</sup>, JianKun Zhu<sup>1</sup>, Zhanfeng Si<sup>1</sup>, Tianzhen Zhang<sup>1</sup>,  
13 Yan Hu<sup>1#</sup>

14

15 <sup>1</sup> Zhejiang Provincial Key Laboratory of Crop Genetic Resources, Institute of Crop Science, Plant  
16 Precision Breeding Academy, College of Agriculture and Biotechnology, Zhejiang University, Zhejiang  
17 310029, China.

18 <sup>2</sup> State Key Laboratory of Crop Genetics and Germplasm Enhancement, Nanjing Agricultural University,  
19 Nanjing 210095, China.

20

21

22

23 \*These authors contributed equally to this work.

24 #Correspondence and requests for materials should be addressed to Dr. Yan Hu (0016211@zju.edu.cn)

This article has been accepted for publication and undergone full peer review but has not been through the copyediting, typesetting, pagination and proofreading process, which may lead to differences between this version and the [Version of Record](#). Please cite this article as [doi: 10.1111/TPJ.15477](https://doi.org/10.1111/TPJ.15477)

This article is protected by copyright. All rights reserved

---

## SUMMARY

The cotton pigment gland is a distinctive structure that functions as the main deposit organ of gossypol and its derivatives. It is also an ideal system in which to study cell differentiation and organogenesis. However, only a few genes that determine the process of gland formation have been reported, including *GoPGF*, *CGPI*, and *CGFs*; the molecular mechanisms underlying gland initiation are still largely unclear. Here, we report discovery of a novel stem pigment gland-forming gene *GoSPGF* by map-based cloning; annotated as a GRAS transcription factor, this gene is responsible for the glandless trait specifically on the stem. In the stem glandless mutant T582, a point mutation (C to A) was found to create a premature stop codon and truncate the protein. Similarly, virus-induced gene silencing of *GoSPGF* resulted in glandless stems and dramatically reduced gossypol content. Comparative transcriptomic data showed that loss of *GoSPGF* significantly suppressed expression of many genes involved in gossypol biosynthesis and altered expression of genes involved in gibberellic acid signaling/biosynthesis. Overall, these findings provide more insight into the networks regulating glandular structure differentiation and formation in cotton, which will be helpful for understanding other plants bearing special gland structures such as tobacco, artemisia annua, mint, and rubber.

**Key words:** *Gossypium hirsutum*, gland-forming gene, map-based cloning, VIGS, stem

---

**SIGNIFICANCE STATEMENT**

A novel cotton gland-forming gene *GoSPGF*, annotated as a GRAS transcription factor, regulates the glandless trait specifically on the stem. The findings concerning *GoSPGF* provide more insight into networks regulating glandular structure differentiation and formation in cotton.

---

## INTRODUCTION

First proposed by Karsten in 1857, lysigenous glands are specialized secretory structures that come about through cell lysis to form secretory cavities and ducts; representative examples are found in *Citrus aurantium* L., *Rhus* L., *Myrtus* L., *Sagittaria* L., *Angiopteris*, *Cycas*, *Pinus*, *Hypericum* L., *Ptelea* L., *Hedera* L., *Thuja* L., *Tilia* L., and *Alisma* L. Cotton pigment glands are ovoid structures derived from lysigenous epidermal cells in the leaves, stems, and bolls of the plant, along with its seeds. The glands appear as black specks because the yellow-green polyphenolic compound gossypol and its derivatives are deposited in them. High amounts of gossypol are toxic to man and to monogastric animals, preventing the commercialization of cottonseed kernels as food and feed for poultry, swine, or horses (Stipanovic *et al.*, 1975). Previous investigations showed gossypol to mainly be synthesized in cotton roots, then transported to and stored in the pigment glands of aerial tissues and organs (Zhao *et al.*, 2020). Consequently, there is a positive relationship between gland density and gossypol content: among different cotton varieties, the number and density of glands serves as an indicator for gossypol content.

To date, extensive research has been conducted with a focus on the morphogenesis and genetic and molecular mechanisms of pigment glands, aiming to cultivate low-gossypol cotton varieties through controlling gland formation. Ultrastructural studies have shown that ontogenesis of the pigment glands originates with a cluster of meristem cells characterized by smaller size, dense cytoplasm, large nuclei, and thin cell walls. As development proceeds, the cytoplasm among the internal cells of this cluster becomes condensed, then the cells degrade gradually through programmed cell death (PCD), finally forming the cavity that we term a cotton gland. Genetic studies on the inheritance of gland traits in allotetraploid upland cotton revealed the pattern of gland distribution on aerial plant parts and seeds to be determined by the combination of at least six independent loci, denoted  $gl_1$ ,  $gl_2$ ,  $gl_3$ ,  $gl_4$ ,  $gl_5$ , and  $gl_6$  (Pauly and Vaissayre, 1980).

Of those loci,  $gl_1$  corresponded to the first genetic locus identified as responsible for gland formation (McMichael, 1954). Plants having the homozygous form of the  $gl_1$  locus ( $gl_1gl_1$ ) display glandless traits only on the stems, petioles, and carpel walls, with leaves and seeds containing normal numbers of glands. Subsequently, two recessive genes,  $gl_2$  and  $gl_3$ , were identified that control the presence of glands in

---

seeds (McMichael, 1960). When doubly recessive for those genes ( $gl_2gl_2gl_3gl_3$ ), all above-ground parts of the plant lack visible glands, including the seeds. Further studies found the monomeric mutants  $2(gl_2Gl_3)$  and  $2(Gl_2gl_3)$  to display different gland distribution patterns. In the  $Gl_2gl_2gl_3gl_3$  genotype, glands distributed most abundantly about the margins and along the midvein of the cotyledon, while in the  $gl_2gl_2Gl_3gl_3$  genotype, glands distributed along the margin of the cotyledon. Meanwhile, plants having the  $gl_2gl_2Gl_3gl_3$  genotype had much lower gland number than those having  $Gl_2gl_2gl_3gl_3$ , indicating that the  $Gl_2$  locus has a more important role in gland formation than the  $Gl_3$  locus. These two recessive genes have been applied in the development of many glandless cultivars of both *G. hirsutum* and *G. barbadense*; however, cultivars containing the double recessive genotype  $2(gl_2gl_3)$  are easily contaminated through spontaneous interspecific hybridization with glanded cotton cultivars, which greatly limits their utilization.

More efficient breeding of low-gossypol cotton cultivars has been achieved with the dominant glandless allele  $Gl_2^e$ , which comes from the glandless line Bahtim 110 developed in Egypt from progeny of Giza 45 that were irradiated with radioactive phosphorous ( $^{32}P$ ). The gene underlying  $Gl_2^e$  was the first to be isolated (by map-based cloning) and experimentally tested (Ma *et al.*, 2016), and was named *GoPGF*; it is a member of the bHLH gene family. In subsequent studies, investigation of differential gene expression between glanded and glandless varieties identified four genes that participate in gland formation and gossypol accumulation: three cotton gland formation (CGF) genes (*CGF1*, *CGF2*, and *CGF3*) and a member of the MYB transcription factor family (*CGP1*) (Janga *et al.*, 2019; Gao *et al.* 2020). Besides these, three additional alleles,  $gl_4$ ,  $gl_5$ , and  $gl_6$ , were also identified in upland cotton; these are relatively weak in expression and have only slight effects on gland presence (Lee, 1962).

Although several cotton genes have been identified as involved in gland formation, the molecular mechanisms responsible for the initial parameters of that process—cell differentiation, formation, distribution pattern, size, and density—still remain largely unknown. In this report, we identified a causative gene in the  $gl_1$  locus that is the first identified allele to control the gland developmental process in the stem. Our result will help unravel not only the networks regulating gland development but also the complex relationship between cotton glands and their secretory or deposited gossypol compounds.

This article is protected by copyright. All rights reserved

---

## RESULTS

### Map-based cloning of *gl<sub>1</sub>* locus

T582 is a multiple-recessive marker line with five mutant genes, including *glandless-1* (*gl<sub>1</sub>*), that were simultaneously introduced into the TM-1 background (**Figure 1A and Figure S1**). Genetic analysis in mapping populations revealed the glandless status of the stem to be controlled by a single recessive gene, due to the respective 3:1 and 1:1 glanded:glandless phenotype segregation ratios in F<sub>2</sub> and BC<sub>1</sub> populations (Zhu *et al.*, 2017). Based on our previous bulked-segregant analysis and sequencing (BSA-seq) using TM-1 v1.0 as the reference genome (Zhang *et al.*, 2015), the *gl<sub>1</sub>* locus was primarily mapped within a 2.05 Mb interval on Chr. D08 (Zhu *et al.*, 2017). In this study, we reanalyzed the BSA-seq data of the *gl<sub>1</sub>* mutant-type bulked pool and TM-1 using as reference the updated cotton genome v2.1 (Hu *et al.*, 2019). Consequently, *gl<sub>1</sub>* was anchored on Chr. D08, ranging from 57.84 and 59.26 Mb and covering a physical region of 1.42 Mb (**Figure 1B and Figure S2**). Within this region, 1,248 SNPs differed between TM-1 and T582 (**Table S1**). Strikingly, only one detected SNP (C to A) located in an exon of *GH\_D08G1984*; this SNP resulted in a premature stop in the mutant T582. Coincidentally, this point mutation also created a new digestion site that could be recognized by the enzyme *Bfa*1(C/TAG) (**Figure 1C**). Based on that observation, 200 F<sub>2</sub> individuals with the glandless trait were selected and subjected to digestion assay with *Bfa*1 to test the relationship between this digestion site (i.e. SNP) and gland status. The results showed that the SNP (C/A) co-separated with stem gland status (**Figure 1D**). To confirm this mapping result, we designed three adjacent SNP markers near the SNP to screen TM-1 and glandless mutants segregated from the mapping populations. Finally, *gl<sub>1</sub>* was successfully narrowed down to within a 114-kb region flanked by the markers k9131 and k9204 (**Figure 1B**). According to the annotation of the reference TM-1 genome, only six putative open reading frames (ORFs) were predicted in this interval, including *GH\_D08G1984* (**Table S2**).

### Comparison of the genomic sequences and expression levels of candidate genes

We validated the expression patterns of these six ORFs using transcriptomic data from 14 tissues of TM-1 (Hu *et al.*, 2019) (**Table S3**). The data showed that three of the six ORFs were expressed (defined as transcripts per million [TPM]>1) in stems. Quantitative real-time PCR analysis further indicated that only *GH\_D08G1984* was

Accepted Article

---

significantly down-regulated in the stem of T582 relative to TM-1 (Student's *t*-test) (**Figure S3**). Full-length coding regions of the six genes were isolated from both TM-1 and T582 and sequenced (**Figure S4**). Alignment of those sequences showed no variation between cultivars in coding regions other than *GH\_D08G1984*, and the observed variation in *GH\_D08G1984* was consistent with the exonic SNP identified by BSA analysis (**Table S1**). Thus, taking together the differences in expression level and genome sequence, *GH\_D08G1984* was considered the candidate gene for the *gl<sub>1</sub>* locus.

### ***GH\_D08G1984*-silenced cotton plants exhibited glandless stems and low gossypol.**

Virus-induced gene silencing (VIGS) is a rapid and effective method for the silencing of a target gene and has been widely used for functional studies in cotton (Ma *et al.*, 2016; Gao *et al.*, 2020). We isolated a specific 301-bp fragment (300~600 bp) at the 3' end of *GH\_D08G1984* from TM-1 and inserted it into the VIGS vector pTRV2 to generate a construct for gene silencing (Qu *et al.*, 2012). Plants with their endogenous expression of *GH\_D08G1984* decreased by VIGS exhibited newly-growing stems that were glandless or had fewer visible glands, while gland abundance on leaves stayed unchanged, suggesting a crucial role for this gene in the regulation of gland formation on stems specifically (**Figure 2A**). Microscopy of transverse sections of *GH\_D08G1984*-silenced plants indicated an absence of gland cavities on the stems (**Figure 2B**). Quantitative real-time PCR (qRT-PCR) confirmed that the expression of *GH\_D08G1984* in stems was significantly lower in T582 and VIGS plants than that in the glanded TM-1 (**Figure 2C**). Similarly, HPLC determined stem gossypol content to be strongly reduced in VIGS plants relative to TM-1, whereas leaf gossypol content remained comparable (**Figure 3A, B**). In addition, genes previously reported to be involved in gland formation and gossypol biosynthesis such as *CAD*, *CYP706B1*, *CYP71BE79*, *CYP82D113*, *2-ODD-1*, and *CGP1* (Tian *et al.*, 2018; Gao *et al.*, 2020) were greatly down-regulated in T582 and VIGS plants (**Figure 3C**). Taken together, all these results strongly demonstrate that *GH\_D08G1984* is the causal gene underlying the *gl<sub>1</sub>* locus that regulates gland formation on the stem, and so is hereafter renamed as *Gossypium STEM PIGMENT GLAND FORMING GENE* (*GoSPGF*).

### **Isolation and functional analysis of *GoSPGF***

This article is protected by copyright. All rights reserved

We cloned *GoSPGF* (*GH\_D08G1984*) and its homologous gene (*GH\_A08G1970*) from TM-1 and T582. Both contain a predicted 2,175-bp open reading fragment (ORF) with 98% sequence identity and no introns, encoding a total of 715 amino acids (**Figure S5**). The deduced amino acid sequence of the *GoSPGF* gene product belongs to the Scarecrow (SCR) subgroup of the GRAS transcription factor family; both amino acid sequences shared 50% similarity to *SCARECROW-LIKE 6* (*SCL6*) in *Arabidopsis* (*AT4G00150*). As demonstrated previously, *SCL6* is absolutely required for proper radial patterning of the root and shoot in *Arabidopsis* (van den Berg *et al.*, 1995, Fukaki *et al.*, 1998).

Sequence alignment of *GoSPGF* and its homolog revealed 41 single nucleotide polymorphisms that result in 23 amino acid differences. Comparing TM-1 and T582, no polymorphic loci were identified in *GH\_A08G1970*, but one SNP was found in the coding sequence (CDS) of *GH\_D08G1984* (*GoSPGF*) (**Figure 1C and Figure S5**). This nucleotide mutation, from cytosine (C) in TM-1 to adenine (A) in T582, occurred at 2,009 bp and produced a TAG stop codon, resulting in premature termination of translation after 669 amino acid residues in T582 (**Figure 1D**). This termination disrupts the highly-conserved GRAS domain in the C-terminal portion of the protein, suggesting that domain is crucial for *GoSPGF* function. Expression of *GoSPGF* and *GH\_A08G1970* in the T582 mutant and TM-1 plants was determined by qPCR. Stem expression of *GoSPGF* was significantly different between T582 and TM-1, but expression of *GH\_A08G1970* was similar (**Figure S6**).

We then queried the cotton genome and identified other three GRAS genes that have high amino acid sequence identity with *GoSPGF*: its homolog *GH\_A08G1970* (96.82% identity) (Fig S4), *GH\_A12G2406* (68.41% identity), and *GH\_D12G2416* (67.77% identity). We performed VIGS analysis against *GoSPGF* and the three additional GRAS genes. As expected, although qRT-PCR analysis indicated significant down-regulation of all four GRAS genes in the silenced groups, only newly-growing stems in *GoSPGF*-silenced plants exhibited the glandless trait (**Figure S7**).

To better understand *GoSPGF* promoter regulation, a 1.2-kb promoter fragment upstream of the *GoSPGF* initiation codon was cloned from TM-1, shuttled into a binary vector, and fused to the glucuronidase (GUS) marker gene to generate a transformation construct. Tobacco plants were transformed using the *Agrobacterium*-mediated method. GUS staining of the several resulting transgenic

---

lines indicated strong expression in the stem (**Figure 1F**), thereby supporting the distinct role of *GoSPGF* in stem tissue.

***GoSPGF* acts upstream of *GoPGF* in regulating gland formation.**

Our previous study used the glandless mutant Hai-1 to identify a key regulatory factor gene, *GoPGF*, in the *Gl<sub>2</sub><sup>e</sup>* locus (Ma *et al.*, 2016). Silencing of *GoPGF* leads to the glandless phenotype throughout the whole plant. To investigate the relationship between *GoSPGF* and *GoPGF*, we detected their gene expression in contexts where each was perturbed. The experimental set with differing levels of *GoPGF* included: T582 (glandless stem), TRV:*GoSPGF* (glandless stem), TRV:00 (wild type), and TM-1 (wild type). In the T582 and TRV:*GoSPGF* backgrounds, *GoPGF* transcripts were significantly decreased, indicating that down-regulation of *GoSPGF* interferes with the transcription of *GoPGF*. The other set consisted of plants with differing *GoPGF* expression, specifically a *GoPGF*-RNAi plant (glandless throughout the plant) and W<sub>0</sub> (transgenic receptor, wild type); these exhibited no significant difference in *GoSPGF* expression, indicating that silencing of *GoPGF* did not alter expression of *GoSPGF*. We also confirmed this result in two *G. barbadense* cultivars, Giza 45 (wild type) and Hai-1 (glandless across the whole plant). Likewise, knockdown of *GoPGF* in *G. hirsutum* acc. W<sub>0</sub> left the relative expression of *GoSPGF* unchanged (**Figure S8**). Based on these results, we speculated that *GoSPGF* acts upstream of *GoPGF* in the pathway governing cotton gland morphogenesis on stems.

***GoSPGF* regulates a set of genes underlying gland formation.**

To identify genes associated with the function of *GoSPGF* in gland formation, we performed transcriptome sequencing (RNA-seq) on stem and root tissue from T582, TM-1, and the VIGS-silenced TRV:*GoSPGF*, obtaining a total of 18 transcriptomes. RNA-seq reads were mapped to the TM-1 genome v2.1 (Hu *et al.*, 2019) to calculate normalized read counts (TPM) for each gene. Taking TPM >1 as the threshold for expression, on average 70% of genes were deemed expressed among a total annotated gene set of 72,761. Principal component analysis (PCA) highlighted transcriptomic differences among the stem and root tissues from each variety; specifically, plotting PC1 (34.7% of variance) and PC2 (13.2% of variance) yielded six clusters (**Figure S9 and Table S4**), suggesting that these samples diverge with respect to both genotype and tissue features.

This article is protected by copyright. All rights reserved

To investigate differentially expressed genes (DEGs) in the stem and root among TM-1, T582, and TRV:*GoSPGF*, we assessed the variant plants against wild-type in four within-tissue comparisons: stem of T582 vs stem of TM-1, stem of TRV:*GoSPGF*-TM-1 vs stem of TM-1, root of T582 vs root of TM-1, and root of TRV:*GoSPGF*-TM-1 vs root of TM-1 (**Table S5-S8**). As shown in **Figure S10A**, when comparing stem tissues against TM-1, there were 974 up-regulated and 766 down-regulated genes in T582, and 254 up-regulated and 757 down-regulated in TRV:*GoSPGF*-TM-1. Meanwhile, comparison of root tissues against TM-1 identified 1,715 up-regulated and 604 down-regulated DEGs in T582, and 921 up-regulated and 455 down-regulated in TRV:*GoSPGF*-TM-1. Plotting these comparisons in a Venn diagram (**Figure S10B**) revealed 264 common DEGs in the stems of T582 and TRV:*GoSPGF*-TM-1, which consisted of 177 down-regulated genes and 87 up-regulated genes.

We speculated that these DEGs might be influenced by the alteration of *GoSPGF* expression. Enrichment analysis using the Kyoto Encyclopedia of Genes and Genomes (KEGG) revealed a large portion of the common down-regulated DEGs to be annotated with biosynthesis of secondary metabolites—sesquiterpenoid, phenylpropanoid, *etc.* (**Figure S10C**). Further Gene Ontology (GO) enrichment analysis revealed these common down-regulated genes as being enriched in oxidoreductase activity, oxidation-reduction process, terpene synthase activity, sesquiterpene synthase activity, (+)-delta-cadinene synthase activity, *etc.* (**Figure S10D**). This suggests a close relationship between gland formation and gossypol biosynthesis; consequently, we further investigated the expression of genes involved in the gossypol biosynthesis pathway. According to a report by Tian (2018), a total of 95 gossypol biosynthesis genes have been identified in TM-1 v2.1 (**Table S9**). We found most such genes to be dramatically down-regulated in stem tissue of the glandless T582 and *GoSPGF*-silenced plants, which is in accordance with the reduced gossypol content observed in their stems (**Figure 3B**). For example, core mevalonate (MVA) pathway genes such as *HMGS* and *HMGR*, gossypol pathway enzyme genes including *DHI* and *2-ODD-1*, and cytochrome P450 family members including *CYP706B1* showed remarkably decreased expression in glandless stems (T582 and TRV:*GoSPGF*-TM-1) as compared to glanded stems (TM-1) (**Figure 4 and Table S9**). Comparing the expression profiles of gossypol genes in stem and root, we observed much higher expression in roots, indicating gossypol biosynthesis to mainly

---

occur in the root (**Figure 4 and Table S9**); this conclusion is consistent with previous reports (Smith, 1961; Zhao *et al.*, 2020).

***GoSPGF* is involved in the gibberellic acid (GA) signal transduction pathway.**

Many reports have shown that GRAS transcription factors play important roles in gibberellin signal response (Ho-Plágaro, *et al.*, 2019; Zhou *et al.*, 2018). As such, we tested the GA<sub>3</sub> content in root, stem, and leaf of stem glandless (T582 and TRV:*GoSPGF*-TM-1) and glanded plants (TM-1) by HPLC. We found that GA<sub>3</sub> content was significantly reduced in glandless compared to glanded stems; furthermore, the transcriptomic data revealed that when *GoSPGF* transcription was reduced, the expression of a series of genes that regulate GA synthesis was altered: decreased for four gibberellin 20-oxidase (GA20ox) genes and increased for nine gibberellin methyltransferase (GAMT) genes (**Figure 5**). In plants, decreased expression of a GA20ox gene causes decreased GA levels and GA deficiency phenotypes (Coles *et al.*, 1999). More recent work has shown that GAMTs encode enzymes (gibberellin methyltransferases) that catalyze methylation of the C-6 carboxyl group of GAs using S-adenosine-L-methionine as a methyl donor (Varbanova *et al.*, 2007). Increased expression of GAMT genes causes decreased levels of bioactive GA<sub>3</sub> and GA precursors, resulting in the lower GA<sub>3</sub> content in T582 and TRV:*GoSPGF*-TM-1 (**Figure 5**).

In summary, our findings suggest *GoSPGF* and *GoPGF* are two key regulator factors of the gland-forming process. It is becoming clear that cotton pigment glands are regulated by a complex gene network. Our current model is that, with *GoSPGF* being involved in the GA signal transduction pathway, when the GA signal transfers to *GoSPGF*, it will enhance expression of downstream genes such as *GoPGF*. Subsequently, *GoPGF* interacts with other proteins such as CGP1 to regulate gland cell differentiation. With the loss of *GoSPGF* function, DELLA proteins bind to suppress its expression (**Figure 6**). In addition, *GoPGF* positively regulates the expression of gossypol biosynthesis genes. Although the networks governing cotton gland morphogenesis and gossypol synthesis are regulated by relatively independent molecular mechanisms, it is clear some cross-talk occurs; when gland development was forestalled, genes involved in gossypol synthesis had their transcriptional activity reduced in response, and gossypol content decreased as well.

## DISCUSSION

This article is protected by copyright. All rights reserved

---

Glandular trichomes are specialized structures on the surface of plant organs, described as “chemical factories” as they secrete or accumulate various substances such as sugars, polysaccharides, mineral salts, resins, proteins, lipids, *etc.* These phytochemicals have important protective functions against various insect pests and some pathogens (Mao *et al.*, 2007, Cai *et al.*, 2010, Celorio-Mancera Mde *et al.*, 2011, Williams *et al.*, 2011, Mellon *et al.*, 2012). In addition, a large number of plant-produced secondary compounds such as resin, nectar, mint, artemisinin, *etc.* are of great commercial value, being utilized as pharmaceuticals, fragrances, flavorings, and more. As such, great interest is focused on improving the production of high-value plant secondary products; however, the molecular gene network regulating the trichome cell differentiation and gland-forming process are yet largely unclear.

Cotton possesses glandular trichomes termed pigment glands because the deposits of gossypol, hemigossypol, and other related sesquiterpene they contain make the glands visible as black dots on cotton leaves, stems, sepals, bract, and elsewhere. Classical genetic studies have indicated the presence or absence, density, and distribution of glands to be controlled by multiple genetic loci. Aside from the gland gene *GoPGF* underlying the *Gl<sub>2</sub><sup>e</sup>* locus, which was isolated by map-based cloning and experimentally tested in our previous research, only a few gland genes have been identified based on the comparative transcriptome analysis of glanded and glandless cotton. In this study, we identified a stem-specific glandless gene *GoSPGF* under the *gl<sub>1</sub>* locus, which is the second gland gene to be isolated via map-based cloning. Our findings proved that *GoSPGF* specifically regulates gland formation in the cotton stem; that is, glands were not produced on stems when *GoSPGF* expression was suppressed by VIGS, but those on other parts of the plant remained normal. We also discovered a close, unidirectional relationship between *GoSPGF* and *GoPGF*: altering expression of *GoSPGF* changed the expression of *GoPGF*, though not the converse. This indicates that *GoSPGF* acts upstream of *GoPGF* in the gland-forming pathway.

Sequence alignment revealed that in the stem glandless mutant T582, a single-nucleotide mutation in the coding region of *GoSPGF* results in a premature stop codon and forms a truncated protein. The consequent early termination of *GoSPGF* translation destroys the integrity of the GRAS domain, thus might influence the protein’s binding to the *GoPGF* promoter. Comparative transcriptome analysis further indicated that alteration of *GoSPGF* expression affects GA biosynthesis and signal transduction. This result is in accordance with a previous report that the

*Arabidopsis* gene *MYC2*, an ortholog of *GoPGF*, could directly interact with DELLA (a key component of GA signaling) and thus affect a set of genes including terpene synthase (TPS) (Hong *et al.*, 2012). Collectively, these findings demonstrate that GA signaling is involved in gland formation. All told, *GoSPGF* is a new cotton gland gene that participates in gland morphogenesis. This original discovery contributes to basic knowledge of glandular structure and development and provides valuable information for further investigating the complicated relationship between glandular structures and their secreted or deposited compounds.

## EXPERIMENTAL PROCEDURES

### Plant materials

Texas 582 (T582) is a multiple-recessive marker line with the same genetic background as TM-1 (Kohel, 1972). It contains five mutant phenotypes including the stem glandless phenotype that is controlled by a recessive gene locus, *gl<sub>1</sub>*. The *GoPGF*-RNAi line is a transgenic line created by silencing *GoPGF* that displays the glandless phenotype throughout the whole plant. Upland cotton (*Gossypium hirsutum*) plants (W<sub>0</sub>, TM-1, T582, and the *GoPGF*-RNAi line) and *Gossypium barbadense* (Linn, Giza 45, and Hai-1) were cultivated in the field at the experimental station of Nanjing Agricultural University (NJAU) in China. In 2005, TM-1 and T582 were crossed at the Jiangpu Breeding Station, Nanjing Agricultural University (JBS/NAU); subsequently, an F<sub>2</sub> mapping population (2,200 individuals) and BC<sub>1</sub> population (419 individuals) were developed. Plant tissues were carefully removed, immediately snap-frozen in liquid nitrogen, and stored at -70°C for DNA and RNA extraction.

### Map-based cloning of the *gl<sub>1</sub>* gene

We extracted DNA from 28 cluster boll individuals from (T582×TM-1) BC<sub>1</sub> progeny and bulked these in an equal ratio to generate a ‘mutant type’ pool, then conducted whole-genome resequencing with the T582 parents (Si *et al.*, 2018). These reads were trimmed with Sickle software and then aligned to the TM-1 reference genome (Hu *et al.*, 2019), with which alignment the *gl<sub>1</sub>* locus was mapped to a 1.42 Mb region. Using F<sub>2</sub> and BC<sub>1</sub> plants with additional molecular markers that were developed in this work based on the TM-1 genome, the *Ghgl<sub>1</sub>* locus was further mapped to a 114 kb region. The cDNA of candidate genes within that region were amplified from TM-1 (AADD) and T582 (AADD) using the primers listed in **Table S10**, and the resulting PCR products were confirmed by Sanger sequencing.

This article is protected by copyright. All rights reserved

---

### qRT-PCR analysis

RNA was extracted from various tissues using the Plant RNA Rapid Extraction Kit (Molfarming, Nanjing, China). Total RNA was then reverse-transcribed to cDNA using a HiScript II Reverse Transcriptase Kit (Vazyme, Nanjing, China). qRT-PCR was carried out on an Applied Biosystems 7500 Fast Real-Time PCR System (Life Technologies, Carlsbad, CA, USA) in a 20- $\mu$ l volume containing 100 ng of cDNA, 4 pM of each primer, and 10  $\mu$ l of AceQ qPCR SYBR Green Master Mix (Vazyme) according to the manufacturer's protocol. The PCR conditions were as follows: primary denaturation at 95 °C for 20 s followed by 40 amplification cycles of 3 s at 95 °C and 30 s at 60 °C. Melting curve analysis was performed to ensure there was no primer-dimer formation. The qRT-PCR primers for gene expression analysis are detailed in **Table S10**. Data were evaluated using the comparative cycle threshold method described by Livak and Schmittgen (Livak and Schmittgen, 2001). Three biological replicates (three samples harvested from three plants, one from each) were performed per reaction, each with three technical replicates (using the same sample). Mean values and standard errors were calculated based on data from three replicates.

### Vector construction and virus-induced gene silencing (VIGS) assay

A 301-bp fragment of *GoSPGF* cDNA corresponding to bases 300 to 600 of the *GoSPGF* gene was amplified by PCR. The resulting product was cloned into pTRV2 to produce a vector referred to as pTRV2:*GoSPGF* (TRV:*GoSPGF*). *Agrobacterium* cells carrying pTRV1 and pTRV2:*GoSPGF* were resuspended in an infiltration medium (10 mM MgCl<sub>2</sub>, 10 mM MES, 200  $\mu$ M acetosyringone) and adjusted to an OD<sub>600</sub> of 1.0. *Agrobacterium* strains containing the pTRV1 and pTRV2:*GoSPGF* vectors were mixed at a ratio of 1:1, then injected into the cotyledons of 30 ten-day-old TM-1 seedlings, which were placed in the dark for 24 hours and then incubated at 23 °C with a 16-hour light/8-hour dark cycle. Empty-vector (TRV:00) transformed plants were used as experimental controls. The *chloroplastos alterados 1* (*CLAI*) gene was used as a marker of the silencing effect (Gao *et al.*, 2011). Photos were taken three weeks after injection, and leaves were collected for expression detection.

### Measurement of gossypol

Gossypol was extracted from stems or leaves of cotton seedlings as previously described (Tian *et al.*, 2018), and isolated and identified as described by Janga *et al.* (2019) and Stipanovic *et al.* (1988). In brief, leaves were frozen using liquid nitrogen

---

and ground into powder. After extraction with acetonitrile:water:phosphoric acid (80:20:0.1) solution, the obtained extract was analyzed using high performance liquid chromatography (HPLC) (Waters E2695, Milford).

#### **Detection of GA content**

GA<sub>3</sub> and GA<sub>4</sub> were purchased from Sigma. Quantitative analysis of plant hormones was performed in accordance with previously reported methods (Pan *et al.*, 2010). Tissues were snap-frozen in liquid nitrogen and ground immediately. After the addition of 4 µl internal standard, the extraction procedure was repeated twice. The combined extract was then concentrated under reduced pressure and combined with 35 mg Sep-Pak Plus C18 Cartridge (Waters). After solid phase extraction, each well was dried under nitrogen for 25 minutes. A portion (4 µl) of the solution was analyzed using an LC-ESI-MS/MS system consisting of an Agilent 1260 HPLC system coupled to an API6500 triple-quadrupole-stage mass spectrometer (Applied Biosystems/MDS Sciex), operated in multiple reaction monitoring mode (Nanjing Convicted-test Technology Co., Ltd, China).

#### **Promoter analysis**

The 1.2-kb fragment upstream of the *GoSPGF* transcriptional start site was cloned and inserted into the pCAMBIA1391 vector to build the construct ProSPGF-GUS with which expression of GUS is driven by the *GoSPGF* promoter. This construct was introduced into *Nicotiana benthamiana* by *Agrobacterium*-mediated transformation. GUS staining of tissues was performed following previously published procedures (Deng *et al.*, 2012).

#### **RNA-seq**

Leaves and stems were collected from TM-1, T582, and TRV:*GoSPGF*-TM-1, with three biological replicates sampled for each tissue. Total RNA was extracted, quantified, and confirmed of good quality (RNA integrity number >8). RNA-seq libraries were constructed and sequenced on an Illumina X-ten sequencer using 2×150 bp reads. A total of 399,951,294 raw paired-end sequenced reads were generated. After adapter trimming and filtering out low-quality reads, 381,089,295 clean reads were obtained (**Table S4**). RNA-seq data analysis was performed as has been previously described by our laboratory (Ma *et al.*, 2016). In brief, clean reads were aligned to the reference TM-1 genome (PRJNA248163) using TopHat 2.1.1, and quantification of gene expression in TPM was performed with Cufflinks version 2.2.1 (<http://cole-trapnell-lab.github.io/cufflinks/>) using the corresponding GTF annotation

This article is protected by copyright. All rights reserved

file. A gene was defined as differentially expressed upon having a minimum of twofold change (TM-1 vs TRV:*GoSPGF*-TM-1 and TM-1 vs T582). PCA, GO, and KEGG enrichment analysis of differentially expressed genes was conducted using Omicshare Cloud Tools (<http://www.omicshare.com/tools>).

#### ACKNOWLEDGEMENTS

This work was financially supported in part by grants National Natural Science Foundation of China (31970320), the Fundamental Research Funds for the Central Universities (2020XZZX004-03) and Leading Innovative and Entrepreneur Team Introduction Program of Zhejiang (2019R01002).

#### CONFLICT OF INTEREST

The authors declare no conflicts of interests.

#### AUTHOR CONTRIBUTIONS

TZ and YH conceptualized and coordinated the project. YZ, CX, LX, LD, JZ, and ZS conducted mapping, cloning and validation through VIGS of the *gl<sub>1</sub>* gene. YH, and YZ wrote the manuscript. All authors discussed results and commented on the manuscript.

#### DATA AVAILABILITY STATEMENT

RNA-seq raw data was deposited at GenBank under BioProject identifier PRJNA722113.

#### SUPPORTING INFORMATION

**Figure S1.** Phenotypes of TM-1, T582, and F<sub>1</sub> progeny.

**Figure S2.** Gene mapping of *gl<sub>1</sub>* genetic loci by BSA-seq and mapping analysis. A threshold of  $-\log_{10}(P) > 100$  was used to identify distinct peaks, marked by red arrows, as regions spanning candidate genes. The *gl<sub>1</sub>* locus was mapped to chr. D08.

**Figure S3.** Relative expression of the selected candidate genes, determined by qRT-PCR. The x axis indicates the tissues sampled (root, stem, and leaf). Data is shown as the mean ( $\pm$ SD) of three experimental replicates; *p*-values were determined by Student's *t*-test (\*\*,  $P < 0.01$ ).

**Figure S4.** Alignment of the base sequences of six candidate genes (*GH\_D08G1983-*

*GH\_D08G1988*) in TM-1 and T582. One SNP in the C-terminal region of *GH\_D08G1984* is the only exonic difference among the six.

**Figure S5.** Alignment of the base and protein sequences of *gl<sub>1</sub>* (*GH\_D08G1984*) and its homolog *gl<sub>1</sub>-A* (*GH\_A08G1970*) in TM-1 and T582. The 41 single nucleotide polymorphisms result in 23 amino acid differences.

**Figure S6.** Relative expression of *GH\_D08G1984* and *GH\_A08G1970* in root, stem, and leaf tissues of TM-1 and T582 as determined by qRT-PCR (\*,  $P < 0.05$ , *t*-test).

**Figure S7.** VIGS experiments targeting *GoSPGF* and three other GRAS genes. (A) Phenotypes after VIGS in stems of TRV:*CLA*, TRV:00 and silenced groups. (B) Expression of the four GRAS genes in seedlings infiltrated with TRV:*CLA*, TRV:00 and silencing constructs. (n=10, \*\*  $P < 0.01$ , *t*-test);

**Figure S8.** Relative expression of *GoSPGF* and *GoPGF* in various backgrounds. (A) Relative expression in gland cultivars (Giza45, TM-1, and TRV:00) and stem glandless cultivars (Hai1, T582, and TRV:*GoSPGF*-TM-1). (B) Relative expression in *GoPGF*-RNAi transgenic lines and W<sub>0</sub>. Data are shown as the mean ( $\pm$ SD) of three experimental replicates; *p*-values were determined by Student's *t*-test (\*\*,  $p < 0.01$ ).

**Figure S9.** Principal component analysis (PCA) plot showing clustering in TM-1, T582, and VIGS-TM-1 transcriptomes.

**Figure S10.** Comparative transcriptomic analysis of stem glandless and glanded plants.

(A) Volcano map of DEGs from four set comparisons: T582 stem vs TM-1 stem, TRV:*GoSPGF*-TM-1 stem vs TM-1 stem, T582 root vs TM-1 root, and TRV:*GoSPGF*-TM-1 root vs TM-1 root. (B) Venn plot depicting counts of overlapping up-regulated and down-regulated genes in the four comparison sets. (C) KEGG-enriched common up- and down-regulated DEGs. (D) Top 20 GO terms of the common up- and down-regulated DEGs.

**Table S1.** Details of SNPs between TM-1 and T582 within the mapping interval.

**Table S2.** Descriptions of candidate genes.

**Table S3.** Expression of candidate genes in several vegetative and reproductive organs.

**Table S4.** Statistics from the sequencing data.

**Table S5.** DEGs in T582 stem vs TM-1 stem.

**Table S6.** DEGs in T582 root vs TM-1 root.

---

**Table S7.** DEGs in VIGS-TM-1 stem *vs* TM-1 stem.

**Table S8.** DEGs in VIGS-TM-1 root *vs* TM-1 root.

**Table S9.** Genes in the mevalonate (MVA) and gossypol pathways.

**Table S10.** All primers developed and used in the present work.

## Figures and their captions

### Figure 1. Cloning of *Ghgl<sub>1</sub>*.

(A) Phenotypes of TM-1, T582, and F<sub>1</sub> progeny. (B) Using the F<sub>2</sub> generation, *Ghgl<sub>1</sub>* was first mapped to the D3 chromosome between the k5607 and k5457 markers. It was then further fine-mapped using extreme populations to the 114-kb interval between k9131 and k9204. Within that region, *GH\_D08G1984* (*Ghgl<sub>1</sub>*) was selected as a major candidate gene. (C) Schematic representation of *Ghgl<sub>1</sub>* DNA and protein sequences. The red rectangle indicates the change from cytosine (C) in TM-1 to adenine (A) in T582; the light grey column boxed with a dotted line represents the GRAS domain in Ghgl1; the dotted black line indicates the loss of the *Ghgl<sub>1</sub>* GRAS domain caused by the 165-bp-early truncation. (D) Genotyping by *Bfa* I digestion in TM-1, T582, and extreme populations. (E) Relative expression of *Ghgl<sub>1</sub>* in root, stem, and leaf tissues of TM-1 and T582 as determined by qRT-PCR. (F) GUS staining of ProSPGF-GUS transgenic tobacco stem apex. Scale bar = 0.5 cm.

### Figure 2. Silencing *Ghgl<sub>1</sub>* reduces pigmented glands on stem.

(A) Stem phenotypes of TM-1, TRV:*CLA*, *chloroplastos alterados 1* positive control, TRV:00 empty vector control, TRV:*Ghgl<sub>1</sub>* silenced, and T582 stem glandless cotton plants. (B) Toluidine blue staining of paraffin sections of TRV:*CLA*, TRV:00, TRV:*Ghgl<sub>1</sub>*, and T582 cotton stems. Cavities indicated by white arrows are the glands. Scale bar = 0.5 mm. (C) Expression of *Ghgl<sub>1</sub>* in T582 and in TM-1 seedlings infiltrated with TRV:*CLA*, TRV:00, and TRV:*Ghgl<sub>1</sub>* (n=20, \*\*  $P < 0.01$ , *t*-test).

### Figure 3. Analysis of gossypol content and the expression of previously reported gland genes in *Ghgl<sub>1</sub>*-silenced TM-1 and T582.

(A) HPLC analysis of gossypol in stems and leaves of TRV:*CLA*, TRV:00, TRV:*Ghgl<sub>1</sub>*, and T582. The gossypol peak is marked with a black arrow. (B) Gossypol content in stems and leaves of TRV:*CLA*, TRV:00, TRV:*Ghgl<sub>1</sub>*, and T582 (n=10, \*\*  $P < 0.01$ , *t*-test). (C) Relative expression levels of gossypol biosynthesis genes in stems of TRV:*CLA*, TRV:00, TRV:*Ghgl<sub>1</sub>*, and T582 (n=10, \*\*  $P < 0.01$ , *t*-test).

### Figure 4. Gossypol pathway enzyme genes and their expression.

This article is protected by copyright. All rights reserved

Genes encoding the enzymes that catalyze defined steps in the mevalonate (MVA) and gossypol pathways and their homologs are shown. The heatmap indicates gene expression, estimated using Stringtie by computing the transcripts per kilobase of exonmodel per million mapped reads (TPM value) for each transcript. Dashed arrows indicate unidentified reaction(s). ACAT, acyl CoA-cholesterol acyltransferase; DMAPP, dimethylallyl diphosphate; FPS, FPP synthase; HMGR, HMG-CoA reductase; HMGS, HMG-CoA synthase; IPP, isopentenyl diphosphate; IPPI, IPP isomerase; MVK, mevalonate kinase; MVP, phosphomevalonate kinase; PMD, diphosphomevalonate decarboxylase; VIGS, *GoSPGF*-VIGS-TM-1 plants. TPM values are listed in **Table S9**.

**Figure 5. Altered *GoSPGF* expression affects GA metabolism.**

Differential expression of GA synthesis genes in TM-1, T582, and TRV:*GoSPGF*-TM-1. CPS, ent-copalyl diphosphate synthase; ER, endoplasmic reticulum; GAMT, gibberellin methyltransferase; GA20ox, GA oxidases; KAO, ent-kaurenoic acid oxidase; KO, ent-kaurene oxidase; KS, ent-kaurene synthase; MT, methyltransferase; 2ODD, 2-oxoglutarate-dependent dioxygenase. Four GA20ox genes are listed in the blue box; nine GAMT genes in the purple box; and bioactive GA3 content in four different experiment groups in the green box (\*\*  $P < 0.01$ , *t*-test).

**Figure 6. Schematic model illustrating the proposed functions of *GoSPGF* and *GhPGF* in cotton gland morphogenesis and pigmentation.**

Gland development is regulated by a complex gene network, with *GoSPGF* being the key regulatory factor for gland morphogenesis in the stem. *GoSPGF* is involved in the GA signal transduction pathway and enhances the expression of its downstream gene *GoPGF*, which can further regulate gland morphogenesis and gossypol production in the stem. Whether *GoSPGF* interacts directly with the promoter of *GoPGF* remains to be determined.

---

**Reference:**

- Cai, Y., Xie, Y. and Liu, J.** (2010) Glandless seed and glanded plant research in cotton. A review. *Agronomy for Sustainable Development*, **30**, 181-190.
- Celorio-Mancera Mde, L., Ahn, S.J., Vogel, H. and Heckel, D.G.** (2011) Transcriptional responses underlying the hormetic and detrimental effects of the plant secondary metabolite gossypol on the generalist herbivore *Helicoverpa armigera*. *BMC Genomics*, **12**, 575.
- Coles, J.P., Phillips, A.L., Croker, S.J., García-Lepe, R., Lewis, M.J. and Hedden, P.** (1999) Modification of gibberellin production and plant development in *Arabidopsis* by sense and antisense expression of gibberellin 20-oxidase genes. *Plant Journal*, **17**, 547-556.
- Deng, F., Tu, L., Tan, J., Li, Y., Nie, Y. and Zhang, X.** (2012) *GbPDF1* is involved in cotton fiber initiation via the core cis-element HDZIP2ATATHB2. *Plant Physiology*, **158**, 890–904.
- Fukaki, H., Wysocka-Diller, J., Kato, T., Fujisawa, H., Benfey, P.N. and Tasaka, M.** (1998) Genetic evidence that the endodermis is essential for shoot gravitropism in *Arabidopsis thaliana*. *Plant Journal*, **14**, 425-430.
- Gao, W., Xu, F., Long, L., Li, Y., Zhang, J., Chong, L. et al.** (2020) The gland localized CGP1 controls gland pigmentation and gossypol accumulation in cotton. *Plant Biotechnology Journal*, **18**(7), 1573-1584.
- Gao, X., Britt, R.C., Jr., Shan, L. and He, P.** (2011) *Agrobacterium*-mediated virus-induced gene silencing assay in cotton. *Journal of Visualized Experiments*. **54**, 2938.
- Ho-Plágaro T, Molinero-Rosales N, Fariña Flores D, Villena Díaz M, García-Garrido JM.** (2019) Identification and expression analysis of GRAS transcription factor genes involved in the control of arbuscular mycorrhizal development in tomato. *Frontiers in Plant Science*, **10**, 268.
- Hong, G.J., Xue, X.Y., Mao, Y.B., Wang, L.J. and Chen, X.Y.** (2012) *Arabidopsis* MYC2 interacts with DELLA proteins in regulating sesquiterpene synthase gene expression. *Plant Cell*, **24**, 2635-2648.
- Hu, Y., Chen, J., Fang, L., Zhang, Z., Ma, W., Niu, Y. et al.** (2019) *Gossypium barbadense* and *Gossypium hirsutum* genomes provide insights into the origin and evolution of allotetraploid cotton. *Nature Genetics*, **51**, 739-748.
- Janga, M.R., Pandeya, D., Campbell, L.M., Konganti, K., Villafuerte, S.T., Puckhaber, L. et al.** (2019) Genes regulating gland development in the cotton plant. *Plant Biotechnology Journal*, **17**, 1142-1153.
- Kohel, R.J.** (1972) Linkage tests in upland cotton, *Gossypium hirsutum* L. II. *Crop Science*, **5**, 66-69.
- Lee, J.A.** (1962) Genetical studies concerning the distribution of pigment glands in the cotyledons and leaves of upland cotton. *Genetics*, **47**, 131.

- Livak, K.J. and Schmittgen, T.D.** (2001) Analysis of relative gene expression data using real-time quantitative PCR and the 2(-Delta Delta C(T)) Method. *Methods*, **25**, 402-408.
- Ma, D., Yan, H., Yang, C., Liu, B., Fang, L., Wan, Q. et al.** (2016) Genetic basis for glandular trichome formation in cotton. *Nature Communications*, **7**, 10456
- Mao, Y., Cai, W., Wang, J., Hong, G., Tao, X., Wang, L. et al.** (2007) Silencing a cotton bollworm P450 monooxygenase gene by plant-mediated RNAi impairs larval tolerance of gossypol. *Nature Biotechnology*, **25**, 1307-1313.
- McMichael, S.C.** (1954) Glandless boll in upland cotton and its use in the study of natural crossing. *Agronomy journal*, **46**.
- McMichael, S.C.** (1960) Combined effects of glandless genes  $gl_2$  and  $gl_3$  on pigment glands in the cotton plant. *Agronomy journal*, **52**, 385-386.
- Mellon, J.E., Zelaya, C.A., Dowd, M.K., Beltz, S.B. and Klich, M.A.** (2012) Inhibitory effects of gossypol, gossypolone, and apogossypolone on a collection of economically important filamentous fungi. *Journal of Agricultural and Food Chemistry*, **60**, 2740-2745.
- Pan, X., Welti, R. and Wang, X.** (2010) Quantitative analysis of major plant hormones in crude plant extracts by high-performance liquid chromatography-mass spectrometry. *Nature Protocol*, **5**, 986-992.
- Pauly, G. and Vaissayre, M.** (1980) Present state of the breeding work on the characters of resistance to boll caterpillars in central Africa. *Coton Et Fibres Tropicales*.
- Qu, J., Ye, J., Geng, Y.F., Sun, Y.W., Gao, S.Q., Zhang, B.P. et al.** (2012) Dissecting functions of KATANIN and WRINKLED1 in cotton fiber development by virus-induced gene silencing. *Plant Physiology*, **160**, 738-748.
- Si, Z., Liu, H., Zhu, J., Chen, J., Wang, Q., Fang, L. et al.** (2018) Mutation of SELF-PRUNING homologs in cotton promotes short-branching plant architecture. *Journal of Experimental Botany*, **69**, 2543-2553.
- Stipanovic, R.D., Altman, D.W., Begin, D.L., Greenblatt, G.A. and Benedict, J.H.** (1988) Terpenoid aldehydes in upland cottons: analysis by aniline and HPLC methods. *Journal of Agricultural & Food Chemistry*, **36**, 509-515.
- Stipanovic, R.D., Bell, A.A., Mace, M.E. and Howell, C.R.** (1975) Antimicrobial terpenoids of Gossypium: 6-methoxygossypol and 6,6'-dimethoxygossypol. *Phytochemistry*, **14**, 1077-1081.
- Smith FH.** (1961) Biosynthesis of gossypol by excised cotton roots. *Nature*, **192**, 888-889.
- Tian, X., Ruan, J., Huang, J., Yang, C., Fang, X., Chen, Z. et al.** (2018) Characterization of gossypol biosynthetic pathway. *Proceedings of the National Academy of Sciences of the United States of America*, **115**, E5410-e5418.
- van den Berg, C., Willemsen, V., Hage, W., Weisbeek, P. and Scheres, B.** (1995) Cell fate in the *Arabidopsis* root meristem determined by directional signalling. *Nature*, **378**, 62-65.
- Varbanova, M., Yamaguchi, S., Yang, Y., McKelvey, K., Hanada, A., Borochoy, R. et al.**

---

(2007) Methylation of gibberellins by *Arabidopsis* GAMT1 and GAMT2. *Plant Cell*, **19**, 32-45.

**Williams, J.L., Ellers-Kirk, C., Orth, R.G., Gassmann, A.J., Head, G., Tabashnik, B.E. et al.**

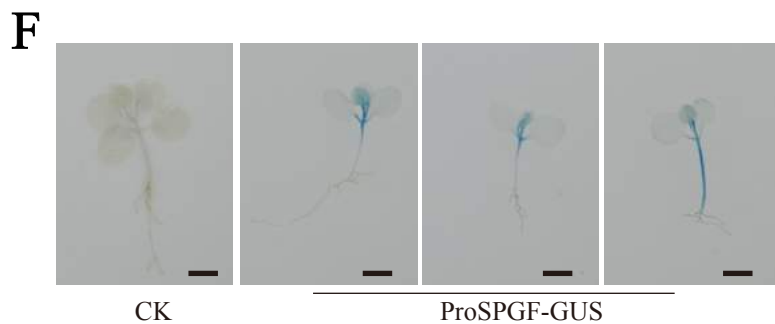
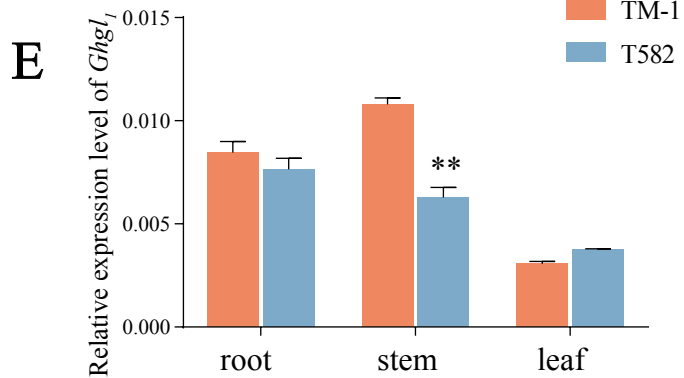
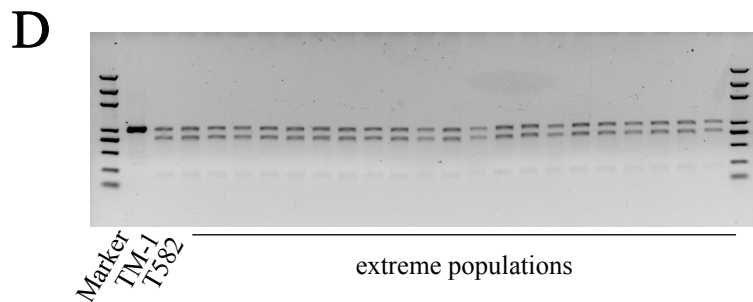
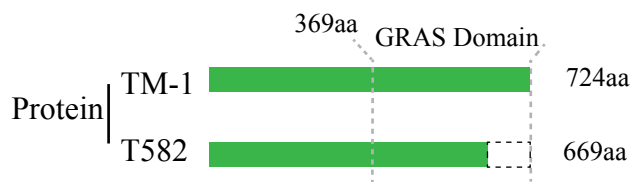
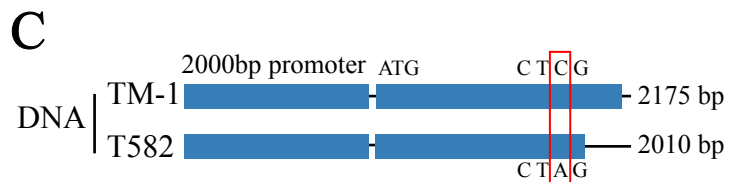
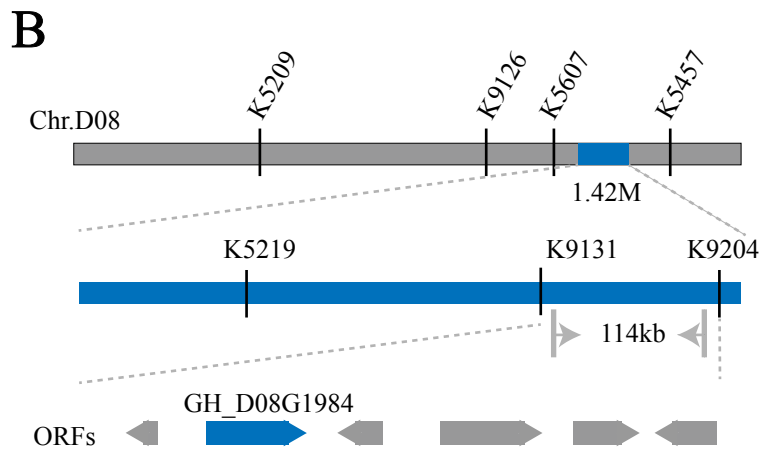
(2011) Fitness cost of resistance to Bt cotton linked with increased gossypol content in pink bollworm larvae. *PLoS One*, **6**, e21863.

**Zhang, T., Hu, Y., Jiang, W., Fang, L., Guan, X., Chen, J. et al.** (2015) Sequencing of allotetraploid cotton (*Gossypium hirsutum* L. acc. TM-1) provides a resource for fiber improvement. *Nature Biotechnology*, **33**, 531-537.

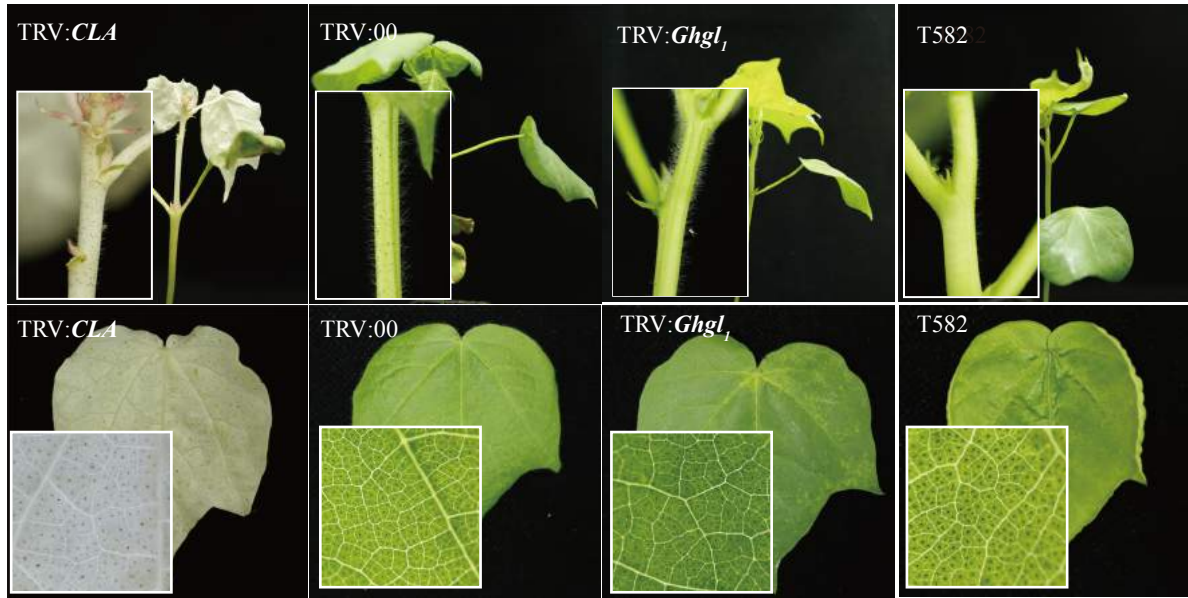
**Zhao, T., Xie, Q., Li, C., Li, C., Mei, L., Yu, J.Z. et al.** (2020) Cotton roots are the major source of gossypol biosynthesis and accumulation. *BMC Plant Biology*, **20**, 88.

**Zhou, S., Hu, Z., Li, F., Yu, X., Naeem, M., Zhang, Y. et al.** (2018). Manipulation of plant architecture and flowering time by down-regulation of the GRAS transcription factor SIGRAS26 in *Solanum lycopersicum*. *Plant Science*, **271**, 81-93.

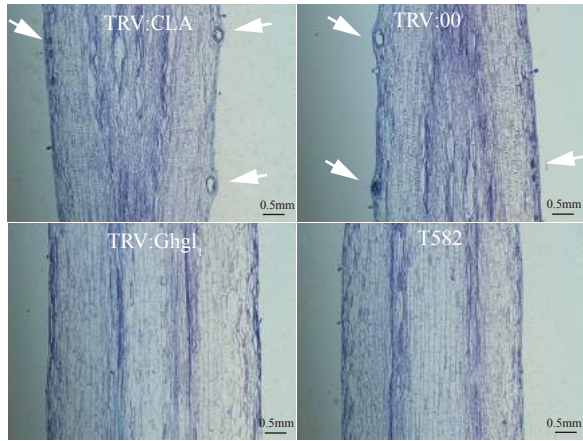
**Zhu, J., Chen, J., Gao, F., Xu, C., Wu, H., Chen, K. et al.** (2017) Rapid mapping and cloning of the virescent-1 gene in cotton by bulked segregant analysis-next generation sequencing and virus-induced gene silencing strategies. *Journal of Experimental Botany*, **68**, 4125-4135.



A



B



C

